





Cite this: *Toxicol. Res.*, 2019, **8**, 297

## Assessment of antioxidant, antibacterial and anti-proliferative (lung cancer cell line A549) activities of green synthesized silver nanoparticles from *Derris trifoliata*

Neethu Cyril,<sup>a,b</sup> James Baben George,<sup>c</sup> Laigi Joseph,<sup>a,d</sup> A. C. Raghavamenon <sup>e</sup> and Sylas V. P. <sup>\*a</sup>

In this work, silver nanoparticles (AgNP-DT<sub>a</sub>) were prepared using an aqueous seed extract of *D. trifoliata*. The importance of the present piece of work is viewed specially with respect to ascertaining the potential of a widely distributed under-utilized mangrove associated plant, *Derris trifoliata* (DT), as medicine. The as-prepared AgNP-DT<sub>a</sub> were well dispersed and stabilised in aqueous solution through biological ligands extracted from the seeds of DT. The functional groups present in the bio-ligands of DT act as reducing and stabilising agents in the formation of nanoparticles. Besides, in the present work, sunlight could induce and catalyse the reduction process of Ag<sup>+</sup> to its corresponding silver atoms of nanoscale dimensions. The size of AgNP-DT<sub>a</sub> decreased with an increase in the duration of sunlight irradiation. Bio-augmented nanoparticles were characterized by UV-vis spectroscopy, XRD, HR-TEM, DLS, AFM and photoluminescence measurements. Preliminary phytochemical studies and FTIR analysis confirmed the presence of secondary metabolites with hydroxyl, amine and carbonyl groups as reducing/capping agents. AgNP-DT<sub>a</sub> demonstrated high DPPH scavenging activity with an IC 50 value of 8.25 μg ml<sup>-1</sup>. Greater antioxidant activity of AgNP-DT<sub>a</sub> was also confirmed from total antioxidant capacity (TAC) assay where it was found that the reducing power of 1 g of AgNP-DT<sub>a</sub> is almost equivalent to that of 1.3 g of Trolox. In addition, highly stable AgNP-DT<sub>a</sub> showed antibacterial activities against Gram positive and Gram negative bacteria. The as-prepared AgNP-DT<sub>a</sub> were observed to inhibit the growth of *Klebsiella pneumonia*, *Staphylococcus aureus* and *Escherichia coli* and no clear zone was obtained for *Pseudomonas aeruginosa*. With reference to the anti-proliferative activities, AgNP-DT<sub>a</sub> exhibited moderate activity on A549 lung cancer cell lines with a median effective concentration of 86.23 ± 0.22 μg ml<sup>-1</sup>.

Received 2nd December 2018,  
Accepted 1st February 2019

DOI: 10.1039/c8tx00323h

rs.c.li/toxicology-research

## 1. Introduction

Rapid progress in the field of nanoscience increases its applications in medical and pharmaceutical sciences. Noble metal nanoparticles exhibit unique properties due to their size, distribution and morphology.<sup>1</sup> Among them silver nanoparticles have been extensively studied and practically applied due to their exclusive biological properties. Previous studies have

reported about the antioxidant,<sup>2,3</sup> antimicrobial,<sup>4–7</sup> anticancer<sup>8</sup> and larvicidal activities<sup>9</sup> of colloidal silver nanoparticles. In the Ayurvedic system of medicine, silver particles in their colloidal state under the name *Rajatha Bhasma* have been used in medicinal formulations in the treatment of various ailments.<sup>10</sup> Several household and medicinal products have incorporated silver for use as an antibacterial agent. Silver nanoparticles acts as a broad-spectrum antimicrobial agent that controls infections from yeast, mold, and bacteria. Recently, conventional technologies have been combined with silver nanoparticle based surface-enhanced Raman spectroscopy (SERS) to develop new nanoparticle probes for cancer detection applications.<sup>11</sup> Studies have shown that silver nanoparticles themselves could act as potential cytotoxic agents against cancer cells.<sup>12</sup>

Synthesis of nanoparticles using biological reducing agents is economical, can easily be scaled up for large scale synthesis, is eco-friendly and does not need high pressure, high tempera-

<sup>a</sup>School of Environmental Sciences, Mahatma Gandhi University, Kottayam, Kerala – 686 560, India. E-mail: sylas@mgu.ac.in, mgubioenergy@gmail.com

<sup>b</sup>Department of Chemistry, Assumption College, Changanassery, Kottayam, Kerala – 686 101, India

<sup>c</sup>Department of Chemistry, St. Berchman's College, Changanassery, Kottayam, Kerala – 686 101, India

<sup>d</sup>Department of Chemistry, Government College, Nattakom, Kottayam, Kerala – 686 013, India

<sup>e</sup>Amala Cancer Research Centre, Amala Nagar, Thrissur, Kerala, 680555, India

ture and toxic chemicals. Microorganisms such as fungi<sup>13</sup> and bacteria,<sup>14</sup> enzymes,<sup>15</sup> plant extracts,<sup>16</sup> proteins,<sup>17</sup> algae<sup>18</sup> and diatoms<sup>19</sup> are being used for the fabrication of nanoparticles. The secondary metabolites present in these biological substrates act as reducing and stabilising agents for the synthesis of nanoparticles.<sup>20,21</sup> In 2014, Xijian Liu *et al.* synthesized a biocompatible photothermal agent based on cysteine-coated CuS nanoparticles for cancer therapy.<sup>22</sup> Amit Kumar Mittal (2015) synthesized AgNPs using a medicinal plant *Potentilla fulgens* Wall. ex Hook with excellent anticancer and antibacterial activities.<sup>23</sup> The blend of photocatalytic and antibacterial properties of algae based AgNPs synthesized using *Chlorella pyrenoidosa* make them useful for waste water treatments.<sup>18</sup> An attractive feature of the biological synthesis is the biocompatibility of the synthesized nanoparticle. In 2011, Nripen Chanda *et al.* have reported the application of biocompatible gold nanoparticles synthesized using cinnamon phytochemicals for phantom CT imaging and photoacoustic detection of cancerous cells.<sup>24</sup> Since the capping agent of nanoparticles is of natural origin, it does not produce much toxic response when exposed to body or bodily fluids. In 2011, Praveen Kumar evaluated the blood compatibility and stability of green synthesised gold nanoparticles of a *Zingiber officinale* extract and found that these nanoparticles were non-platelet activating, non-complement activating and highly stable on contact with whole human blood and thus suggested to use them as vectors for various biomedical applications.<sup>25</sup> These biocompatible green synthesized nanoparticles could find many potential applications especially in cancer diagnosis and therapy, drug delivery, and gene delivery or as biosensors.

*Derris trifoliata* Lour, belonging to the family *Leguminosae*, is one of the common liana occurring along mangrove and coastal regions of Asia and Africa. The seeds are mostly disc-like and one or two seeded, rounded on the lower side, and narrowly winged on the upper side. Its brown seeds are compressed, wrinkled and kidney-shaped. *Derris trifoliata* (DT) is known to contain a large number of bioactive compounds such as flavonoids, alkaloids, steroids and fatty acids. Many unusual flavonoids and related compounds were isolated from different parts of DT. Rotenone, deguelin, dehydrodeguelin, dehydrorotenone, 12a-hydroxy rotenone, tephrosin, 12- $\alpha$ , $\beta$  hydroxyrot-2'-enonic acid, kaempferol-3-O- $\alpha$ -l-rhamnopyranosyl-(1 $\rightarrow$ 6)- $\beta$ -D-glucopyranosyl-(1 $\rightarrow$ 3)- $\beta$ -D-glucopyranoside, spiro-13-homo-13-oxaelliptone, daidzein, 7a-O-methylelliptonol, tachioside and lupinifolin<sup>26–30</sup> are some among the list of flavonoids isolated from *Derris trifoliata*. It is reported that the phytoconstituents present in the *Derris* species are used for antitumor drug formulations, as antiplasmodial, antibacterial and larvicidal agents.<sup>31</sup> In this work we report a one-step method for the synthesis of silver nanoparticles using the aqueous seed extract of *Derris trifoliata* (AgNP-DT). These bio-augmented nanoparticles and aqueous seed extract of DT were evaluated for their antioxidant and anti-bacterial activities. In addition, the anti-proliferative effect of the as-prepared, green synthesized AgNP-DT was also investigated on A549 lung cancer cell lines.

## 2. Materials and methods

Seeds of DT were collected from Vembanad–Kol Ramsar site, Kerala, India. Silver nitrate (AgNO<sub>3</sub>, ACS reagent,  $\geq$ 99.0%, molecular weight (M.wt): 169.87), 1,1-diphenyl-2-picrylhydrazyl radical (DPPH, M.wt: 394.32), Folin–Ciocalteu reagent, sodium carbonate (M.wt: 105.99), potassium acetate (M.wt: 98.14), aluminum chloride (anhydrous powder, 99.999% trace metals basis, M.wt: 133.34), sodium dihydrogen phosphate (M.wt: 141.96), ammonium molybdate (99.98% trace metals basis, M.wt: 196.01), penicillin–streptomycin solution (10 000 units penicillin and 10 mg ml<sup>-1</sup> streptomycin in 0.9% NaCl, sterile-filtered, bio-reagent), amphotericin B solution (M.wt: 924.079) and methylthiazolyldiphenyl-tetrazolium bromide (MTT, 98%, M.wt: 414.32) were procured from Merck India Ltd and used without further purification. All aqueous solutions were prepared using double distilled water. Bacterial cultures were procured originally from the School of Biosciences, M.G. University and Kerala, India. Young cultures of *Escherichia coli* (MTCC 723), *Klebsiella pneumoniae* (MTCC 109) and *Pseudomonas aeruginosa* (MTCC 424) were used for the study. Cancer cell line A549 was procured from the National Centre for Cell Sciences (NCCS), Pune, India.

### 2.1 Synthesis and characterisation of AgNP-DT

10 g of seed powder was extracted with 50 ml of distilled water for 30 minutes and filtered. 1 ml of seed extract was then added to 20 ml of 1 mM solution of AgNO<sub>3</sub> and kept under direct sunlight without stirring. The intensity of incident sunlight radiation varied between 88 800 and 115 000 lux. The above experiment was repeated at room temperature under the same experimental conditions in the absence of sunlight. Bio-functionalized nanoparticles were characterized by various spectroscopic and microscopic techniques. UV-visible studies were carried out using a Shimadzu UV-1700 Pharmaspec spectrophotometer. The IR spectra were recorded using a Shimadzu IR Prestige-21 FTIR spectrometer. X-ray diffraction (XRD) analysis was performed using a Mini Flex 600-Rigaku diffractometer. Photoluminescence studies were carried out using a Horiba-Fluorolog 3 spectrofluorometer. The size and morphology of nanoparticles were examined using a JEOL – Model JEM-2100 high resolution transmission electron microscope (HRTEM). A WITec Atomic Force Microscope (AFM) was used for imaging nanoparticles at the nanoscale. Dynamic Light Scattering (DLS) measurements were carried out using a Litesizer™ 500 Anton Paar GmbH analyser.

### 2.2 Preliminary phytochemical analysis and determination of the total phenolic content of DT

The presence of phytochemical constituents in the aqueous seed extract of DT were analysed by the following standard phytochemical tests.

**2.2.1 Alkaloids.** *Dragendorff reagent test:* The aqueous extract (1 ml) is mixed with 10% acetic acid in ethanol in a test tube and drops of Dragendorff reagent are added. A reddish

orange precipitate indicates the presence of alkaloids in the extract.<sup>32</sup>

**2.2.2 Flavonoids.** *Alkaline reagent test:* 1 ml of aqueous extract is mixed with 10% NaOH solution in a test tube. A deep yellow colouration which disappears with the addition of dilute HCl indicates the presence of flavonoids.<sup>33</sup>

**2.2.3 Saponins.** *Froth test:* 1 ml of extract is heated to boiling with 5 ml distilled water in a test tube. It is then further diluted with 3 ml distilled water and shaken vigorously. Frothing, which persists on warming, indicates the presence of saponins.<sup>34</sup>

**2.2.4 Proteins.** *Ninhydrin test:* 2 ml of extract is taken in a test tube, a few drops of 2% ninhydrin reagent are added, and the solution is mixed thoroughly and heated in a water bath for 5 minutes. A blue colour indicates the presence of proteins in the extract.<sup>35</sup>

**2.2.5 Cardiac glycosides.** *Keller Killiani test:* 2 ml of plant extract is mixed with 2 ml of glacial acetic acid containing 2 drops of 2% FeCl<sub>3</sub> solution. Concentrated H<sub>2</sub>SO<sub>4</sub> is added slowly along the sides of the test tube. A brown ring formation between the layers indicates the presence of cardiac steroidal glycosides.<sup>36</sup>

**2.2.6 Tannins.** *Lead acetate test:* To 1 ml of aqueous extract, a few drops of 10% lead acetate solution are added. Yellow precipitate formation indicates the presence of tannin.<sup>37</sup>

**2.2.7 Determination of the total phenolic content of the aqueous extract.** The total phenolic content of the aqueous extract of DT was estimated by the Folin–Ciocalteu method<sup>38</sup> with gallic acid as the standard solution. Total phenolic assay was conducted by mixing 500 µl of the extract with 2 ml of 10% Folin reagent and finally neutralized with 4 ml of 7.5% sodium carbonate solution. The mixture was incubated at room temperature for 30 minutes with shaking at intervals and the absorbance was measured at 765 nm. A standard curve was prepared with gallic acid. Final results were given as mg per g gallic acid equivalents (GAE) of the dry extract.

### 2.3. Antioxidant activities of AgNP-DTα

**2.3.1 DPPH scavenging activity.** DPPH radical scavenging activity was measured according to the method of Aquino *et al.*<sup>39</sup> DPPH in its radical form has an absorption maximum at 515 nm, which would disappear in the presence of an antioxidant compound. 3 mg of DPPH was dissolved in 25 ml methanol. Different concentrations of the aliquots of AgNP-DTα were added to 187 µL of freshly prepared DPPH. The final volume of the solution was diluted to 1 ml with methanol. The absorbance values for different concentrations of the extract were measured spectrophotometrically at 515 nm after an incubation time of 30 minutes. Each concentration was tested in duplicate. The radical scavenging activity of extracts was expressed in terms of percentage inhibition.

$$\% \text{ Inhibition} = \frac{\text{Absorbance of control} - \text{Absorbance of sample}}{\text{Absorbance of control}} \times 100$$

**2.3.2 Total antioxidant capacity.** This assay is based on the reduction of Mo(vi) to Mo(v) by the extract resulting in the formation of a green coloured phosphomolybdenum complex at an acidic pH.<sup>40</sup> 50 ml of a reagent solution was prepared by mixing 0.247 g ammonium molybdate and 0.168 g of sodium dihydrogen phosphate with 1.6 ml of 0.6 M sulphuric acid. 50 µL of AgNPs was added to 1 ml of the reagent solution and incubated at 95 °C for 90 minutes. After the mixture was cooled to room temperature, the absorbance was taken at 695 nm against the blank. Trolox was used as the standard and the total antioxidant capacity is expressed as mg per g equivalents of Trolox.

### 2.4. Antibacterial assay of AgNP-DTα

The antibacterial assay of AgNP-DTα was performed by the agar well diffusion method.<sup>41</sup> In the assay, nutrient agar plates were swabbed with young cultures of *Escherichia coli* (MTCC 723), *Klebsiella pneumoniae* (MTCC 109), *Pseudomonas aeruginosa* (MTCC 424) and *Staphylococcus aureus* (MTCC 96). Analysis was done in triplicate. Five wells of 6 mm were made in the agar plates. A solution of 0.015 mg AgNO<sub>3</sub>, 0.01 mg AgNP-DTα, 0.02 mg AgNP-DTα, 0.03 mg AgNP-DTα and aqueous seed extract was added to the wells 1, 2, 3, 4 and 5, respectively. The zone of inhibition was measured after 24 hours of incubation.

### 2.5. In vitro antiproliferative activity of AgNP-DTα

MTT [3-(4,5-dimethylthiazol-2-yl)-2,5-diphenyltetrazolium bromide] assay was employed for the evaluation of the antiproliferative activity of AgNP-DTα on human lung carcinoma cell line, A549. The cell line was cultured in a 25 cm<sup>2</sup> tissue culture flask with DMEM (Dulbecco's Modified Eagle's Medium) supplemented with 10% FBS, L-glutamine, sodium bicarbonate and an antibiotic solution containing penicillin (100 U ml<sup>-1</sup>), streptomycin (100 µg ml<sup>-1</sup>) and amphotericin B (2.5 µg ml<sup>-1</sup>). The cultured cell lines were kept at 37 °C in a humidified 5% CO<sub>2</sub> incubator (NBS Eppendorf, Germany). A two days old confluent monolayer of cells were trypsinized and the cells were suspended in 10% growth medium. 100 µl cell suspension (5000 cells/well) was seeded in 96 well tissue culture plates and incubated at 37 °C in a humidified 5% CO<sub>2</sub> incubator. 1 mg of AgNP-DTα was added to 1 ml of DMEM and dissolved completely using a cyclomixer. After that the solution was filtered through a 0.22 µm Millipore syringe filter to ensure the sterility.

After attaining sufficient growth of the cells, the growth medium was removed, freshly prepared samples in 5% DMEM were five times serially diluted by two-fold microdilution (100 µg, 50 µg, 25 µg, 12.5 µg, and 6.25 µg in 100 µl of 5% DMEM) and each concentration of 100 µl was added in triplicate to the respective wells and incubated at 37 °C in a humidified 5% CO<sub>2</sub> incubator. 15 mg of MTT was reconstituted in 3 ml PBS until completely dissolved and sterilized by filter sterilization.

After 24 hours of incubation period, the sample contents in wells were removed and 30 µl of reconstituted MTT solution

was added to all test and cell control wells, the plate was gently shaken well, and then incubated at 37 °C in a humidified 5% CO<sub>2</sub> incubator for 4 hours. After the incubation period, the supernatant was removed and 100 µl of MTT solubilisation solution (DMSO) was added and the wells were mixed gently by pipetting up and down in order to solubilize the formazan crystals. The absorbance values were measured using a microplate reader at a wavelength of 570 nm.

The percentage cell viability was calculated using the formula:

$$\% \text{ cell viability} = \frac{\text{Mean OD of Samples} \times 100}{\text{Mean OD of control group}}$$

The experiment was repeated thrice. After an incubation period of 24 hours, the cytotoxicity was directly observed using an inverted phase contrast tissue culture microscope (Olympus CKX41 with Optika Pro5 CCD camera) and the microscopic observations were recorded as images.

### 3. Statistical analysis

The results of the biological studies were expressed as mean  $\pm$  standard deviation.

## 4. Results and discussion

### 4.1 Synthesis and characterisation of AgNP-DT<sub>a</sub>

Upon sunlight irradiation, the colour of AgNO<sub>3</sub> solution containing the aqueous seed extract changed from colourless to yellowish brown (Fig. 1). This colour change occurred within 2 minutes after the exposure to sunlight. This colour change was due to the formation of silver nanoparticles (AgNP-DT<sub>a</sub>) bio-augmented with ligand molecules from the aqueous seed extract of DT. In the absence of sunlight *i.e.*, at room temperature, the above reaction process was very slow and it took a minimum of 48 hours for the formation of silver nanoparticles. This confirms the catalytic behaviour of sunlight in the reduction of silver ions to the nanoscale using the aqueous seed extract of DT. For the formation of AgNP-DT<sub>a</sub>, the

optimum intensity of incident sunlight radiation was found to be between 88 800 and 115 000 lux. The UV-vis spectra showed no considerable increase in the intensity of peaks after 2 hours which indicates the completion of the reaction. After 2 hours, the synthesized AgNP-DT<sub>a</sub> show an absorption maximum centred at 419 nm. From Fig. 2a, it could be seen that the absorption maximum undergoes a blue shift with an increase in the duration of sunlight irradiation. This blue shift may be due to the formation of small sized nanoparticles. The inset of Fig. 2a shows the gradation in colour with time which might be due to the formation of more number of nanoparticles.

The XRD data of AgNP-DT<sub>a</sub> are shown in Fig. 2b. Diffraction peaks were observed at 38°, 44.86°, 64.70° and 77.4° and matched with standard JCPDS file number 87-0720 and they correspond to (111), (200), (220) and (311) planes of a face centred cubic (fcc) structure of silver crystals. The peaks denoted by \* in the XRD data were due to the crystallization of bioorganic phases that occur on the surface of nanoparticles.<sup>42</sup> The average size of these nanoparticles could be estimated from the Debye-Scherrer equation,

$$\text{Particle size } (D) = \frac{k \times \lambda}{\beta \times \cos \theta}$$

where  $k$  is the Scherrer constant (0.9 for spherical crystals),  $\lambda$  is the wavelength of X-ray ( $\lambda = 0.154$  nm),  $\beta$  is the full width at half maximum (FWHM) and  $\theta$  is the diffraction angle. The average size of AgNP-DT<sub>a</sub> calculated from XRD measurements was  $16.05 \pm 5.0$  nm. Moreover, the lattice constant ( $a$ ) in the fcc unit cell structure of AgNP-DT<sub>a</sub> could be obtained from the XRD pattern by calculating the interplanar spacing ( $d$ ) between adjacent planes on a family ( $hkl$ ), where  $h$ ,  $k$  and  $l$  are the Miller indices. From Bragg's equation,  $\lambda = 2d \sin \theta$ , the interplanar distance ( $d$ ) between (111) planes, where  $2\theta = 38^\circ$ , was found to be 0.2355 nm. Applying the geometric relationship,  $d_{111} = \frac{a}{\sqrt{1^2 + 1^2 + 1^2}}$ , the lattice constant ( $a$ ) in the fcc unit cell structure of AgNP-DT<sub>a</sub> was calculated to be 0.4078 nm.

The photo-physical properties of the green synthesized AgNP-DT<sub>a</sub> were studied using spectrofluorometry. Noble metal nanoclusters composed of only a few atoms have shown very



Fig. 1 (a) DT seeds (<http://www.NatureLoveYou.sg>), (b) AgNO<sub>3</sub> solution, (c) aqueous seed extract and (d) brownish-yellow AgNP-DT<sub>a</sub> nanoparticles.



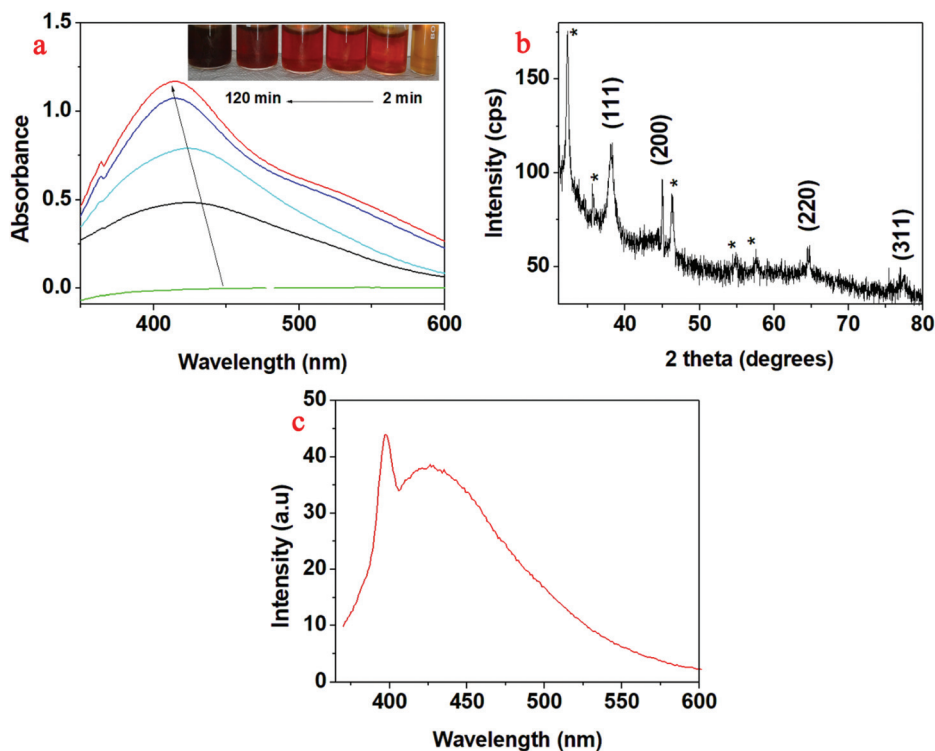


Fig. 2 (a) UV-vis spectra of AgNP-DTAs; inset of (a) shows the gradation in colour with the irradiation time. (b) XRD pattern of AgNP-DTAs and (c) PL emission at 360 nm.

strong and size-dependent emission. In 2002, Zheng and Dickson reported that only the silver clusters formed by photo-reduction could yield strong fluorescence, while the larger nanoparticles formed through reduction with  $\text{NaBH}_4$  were essentially non-fluorescent.<sup>43</sup> The synthesized AgNP-DTAs exhibited strong blue fluorescence under UV light. AgNP-DTAs were excited at 360 nm wavelength and the corresponding double emissions were observed at 396 nm and 505 nm (Fig. 2c). In the case of silver nanoparticles the photo-induced luminescence process includes the excitation of electron-hole pairs, relaxation of the excited electrons and radiative recombination of electrons from the sp band above the Fermi level and holes from the d-band below the Fermi level.<sup>44</sup> Although water is known to quench Ag nanocluster fluorescence,<sup>45</sup> bio-capped AgNP-DTAs are quite stable and fluorescent in aqueous solution. Therefore, the photochemically produced AgNP-DTAs are shielded inside the biological ligands from DT, thereby preventing the interaction with quenchers in the solution. Thus, the fluorescence properties of the AgNP-DTAs imply the possibility of their use in the field of laser technology.

Fig. 3a and b show the FTIR spectra of aqueous extracts of DT and AgNP-DTAs, respectively. A broad and strong peak at  $3333\text{ cm}^{-1}$  in the FTIR spectrum of the aqueous extract could be attributed to  $-\text{OH}$  stretching vibrations of secondary metabolites such as flavonoids, saponins and other phenolic compounds.<sup>46</sup> The band at  $1632\text{ cm}^{-1}$  could be assigned to carbonyl ( $\text{C}=\text{O}$ ) stretching in the carboxyl group (amide I band) of proteins.<sup>47</sup>

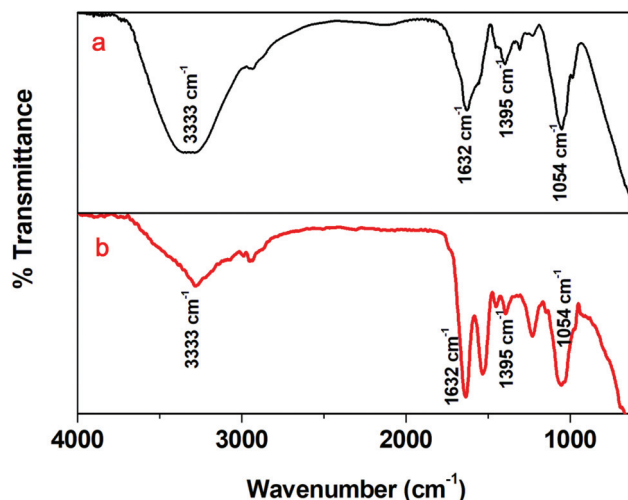


Fig. 3 (a) FTIR spectrum of the DT extract and (b) FTIR spectrum of AgNP-DTAs.

The peak at  $1402\text{ cm}^{-1}$  corresponds to the geminal methyl group of secondary metabolites in the aqueous seed extract.<sup>48</sup> The band at  $1054\text{ cm}^{-1}$  in the FTIR spectrum of the aqueous extract corresponds to  $\text{CN}^-$  stretching in amines.<sup>49</sup> The presence of similar FTIR peaks at  $3333\text{ cm}^{-1}$ ,  $1632\text{ cm}^{-1}$ ,  $1402\text{ cm}^{-1}$  and  $1054\text{ cm}^{-1}$  in the spectrum of AgNP-DTAs confirms the capping of secondary metabolites on the surface of nanoparticles.

The morphology of the AgNP-DT<sub>a</sub> was confirmed by high resolution TEM analysis (Fig. 4a–c). It is evident from the images that nanoparticles are almost spherical in shape and polydispersed. Fig. 3c presents a magnified image of a single AgNP-DT<sub>a</sub>. The highly crystalline nature of as-prepared silver nanoparticles can be clearly evident from their well resolved lattice planes. Selected area electron diffraction (SAED) patterns of the nanoparticles corresponding to Bragg's reflections are shown in Fig. 4d. The average particle size of AgNP-DT<sub>a</sub> calculated from the SAED patterns is  $16.92 \pm 7$  nm. Fig. 4e shows a typical AFM image of AgNP-DT<sub>a</sub>. The average particle size obtained from the AFM measurements was found to be larger than the size calculated from XRD and TEM patterns. This may be due to the intrinsic enlarging effect of the microscopic pinpoint to the measured AgNP-DT<sub>a</sub> nanoparticles, resulting in the observation of a larger particle size using AFM. From DLS measurements, bio-capped AgNP-DT<sub>a</sub> nanoparticles exhibited a zeta potential value of  $-21.0$  mV and were found to be stable at room temperature for more than 3 months without any colour change or aggregation. In the present work, all the biological properties were evaluated by using freshly prepared AgNP-DT<sub>a</sub> synthesized under 2 hour sunlight irradiation.

#### 4.2 Preliminary phytochemical analysis and determination of the total phenolic content of DT

Preliminary phytochemical analysis of the aqueous seed extract of *D. trifoliata* confirmed the presence of secondary

metabolites such as alkaloids, flavonoids, proteins, saponins, glycosides, polyphenols and proteins. Tannins were absent in the extract. The total polyphenolic content in the extract was found to be 58 mg GAE per g dry weight. Some of these polyphenolic compounds and other secondary metabolites in the seed extract might act as strong reducing agents and could reduce Ag<sup>+</sup> ions in the aqueous solution to the Ag<sup>0</sup> state. A number of studies have been reported on the bioactivity of secondary metabolites in plants especially of phenolic compounds.<sup>50–54</sup> The lone pair of electrons in the secondary metabolites could transfer to Ag<sup>+</sup> ions and reduce them to Ag<sup>0</sup>. Sunlight could catalyse the above reaction by increasing the rate of electron transfer from phenolic oxygen to Ag<sup>+</sup> ions.

#### 4.3 Antioxidant activities of AgNP-DT<sub>a</sub>

*In vitro* antioxidant properties of AgNP-DT<sub>a</sub> were evaluated based on DPPH assay and TAC (total antioxidant activity) by phosphomolybdate assay.

**4.3.1 DPPH scavenging activity.** The DPPH method was employed for measuring the free radical capturing ability of the aqueous extract and the synthesized AgNP-DT<sub>a</sub>. This assay is based on the capability of stable free radical 2,2-diphenyl-1-picrylhydrazyl to react with hydrogen donors.<sup>55</sup> A graph was plotted between % inhibition of DPPH against the concentration of AgNP-DT<sub>a</sub> (Fig. 5). From the graph, it was observed that the DPPH scavenging ability of the aqueous seed extract of *DT* and synthesized AgNP-DT<sub>a</sub> showed IC 50 values of  $332.44 \mu\text{g ml}^{-1}$  and  $8.25 \mu\text{g ml}^{-1}$ , respectively.

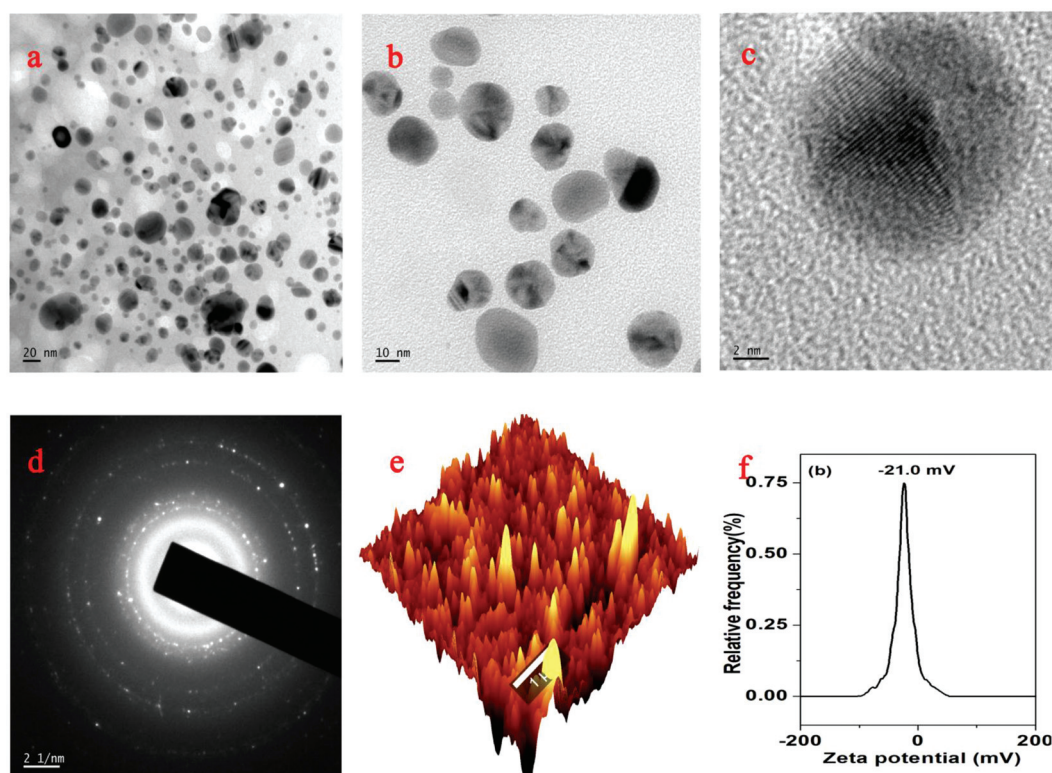


Fig. 4 (a), (b) and (c) TEM images of AgNP-DT<sub>a</sub>, (d) SAED pattern of AgNP-DT<sub>a</sub>, (e) AFM image of AgNP-DT<sub>a</sub> and (f) zeta potential of AgNP-DT<sub>a</sub>.

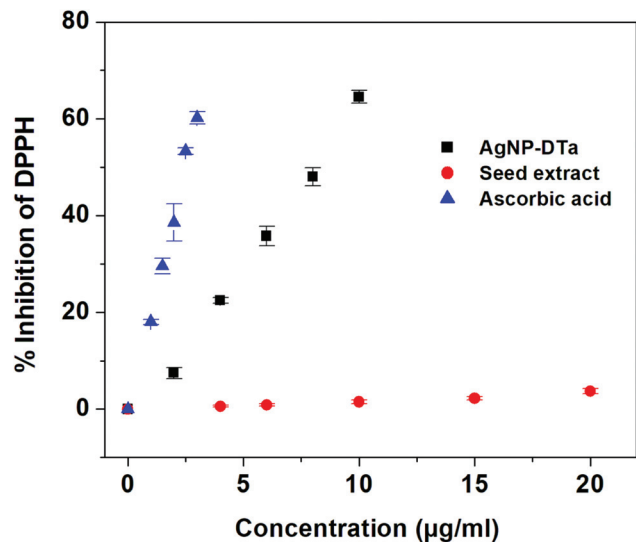


Fig. 5 Percentage inhibition of DPPH radicals with the concentrations of AgNP-DTα, seed extract and ascorbic acid.

Ascorbic acid exhibited an IC<sub>50</sub> value of 2.48 µg ml<sup>-1</sup>. Therefore, AgNP-DTα exhibited strong DPPH scavenging activity compared to other reported green synthesized silver nanoparticles.<sup>56,57</sup> DT is reported to be a rich source of flavonoids.<sup>26,28</sup> However, DPPH does not react with flavonoids, which contain no -OH groups in the B-ring,<sup>58</sup> which might be the reason for the reduced DPPH scavenging activity of the aqueous seed extract of DT.

**4.3.2 Total antioxidant capacity (TAC).** The total antioxidant capacity (TAC) of the aqueous extract and AgNP-DTα was also evaluated using the phosphomolybdenum method. The phosphomolybdenum method is based on the reduction of Mo(vi) to Mo(v) by the extract/AgNP-DTα resulting in the formation of a green coloured phosphomolybdenum complex. Higher reducing power was shown by the synthesized AgNP-DTα (1328.9 ± 20.59 mg g<sup>-1</sup> TE) than the aqueous seed extract (114.4 ± 8.2 mg g<sup>-1</sup> TE). Results showed that the reducing power of 1 g of AgNP-DTα and 1.0 g of aqueous seed extract is equivalent to 1328.9 mg and 114.4 mg of Trolox, the reference compound, respectively. Therefore it could be concluded that AgNP-DTα synthesized from DT have an even greater antioxidant potential than Trolox.

In the above assays, the synthesized AgNP-DTα exhibited significantly high antioxidant activity than the aqueous seed extract of DT. It has been reported in the literature that the antioxidant properties of green synthesized AgNP-DTα could be attributed to the functional groups adhered to them which originated from the plant extract.<sup>59</sup> But in our study the antioxidant potential of AgNP-DTα was higher than that of its extract. A similar observation was obtained for S. Francis *et al.* for the DPPH scavenging activity of microwave assisted green synthesized silver nanoparticles using a leaf extract of *Elephantopus scaber*.<sup>60</sup> Hence it could be concluded that the

antioxidant potential of the as-prepared AgNP-DTα might be not only due to the presence of capped functional groups but also due to their unique size to volume ratio. Generally, the smaller the particle size, the larger will be the surface area. The as-prepared AgNP-DTα with a small size and large specific surface area could therefore provide a lot of active sites to scavenge the free radicals and inhibit the oxidation reactions.<sup>61,62</sup>

#### 4.4. Antibacterial assay of AgNP-DTα

*In vitro* antibacterial activity of the aqueous seed extract of DT and the green synthesized AgNP-DTα were examined against four pathogens such as *Klebsiella pneumoniae*, *Staphylococcus aureus*, *Escherichia coli* and *Pseudomonas aeruginosa* (Fig. 6). The zone of inhibition was measured and compared between various concentrations (Table 1). The zone of inhibition increased with the increase in the concentration of AgNP-DTα. In order to recognize the effect of the natural stabilizer from DT, antibacterial tests of the newly synthesized AgNP-DTα and of the aqueous seed extract of DT were performed. All of these antibacterial activity assays were performed according to the above-mentioned method. The obtained results revealed that the aqueous seed extract of DT, at the tested concentration, did not show any zone of inhibition indicating less antibacterial activity. Thus the antibacterial activity of the system was merely due to AgNP-DTα and not its stabilising agent. The antibacterial activity of AgNP-DTα can be attributed to the ability of ligands of DT to stabilize the nanoparticles against

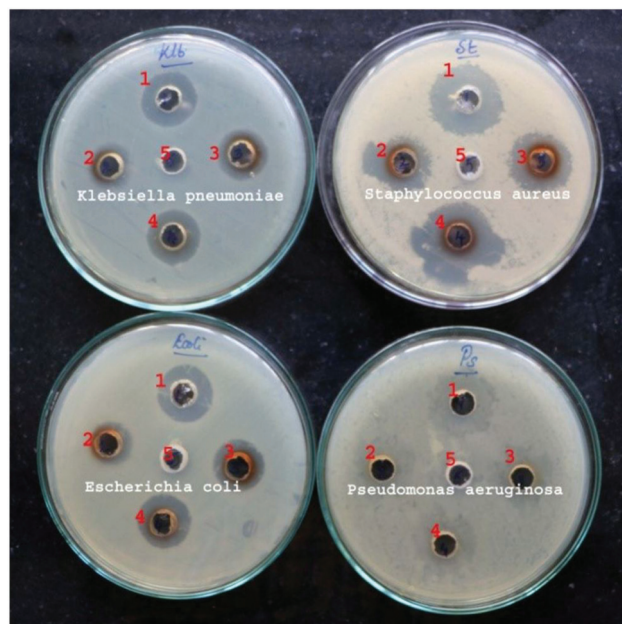


Fig. 6 (a) Photographs of the antimicrobial plates of *Klebsiella pneumoniae*, *Staphylococcus aureus*, *Escherichia coli* and *Pseudomonas aeruginosa*; 1, 2, 3, 4 and 5 contain 0.015 mg AgNO<sub>3</sub>, 0.01 mg AgNP-DTα, 0.02 mg AgNP-DTα, 0.03 mg AgNP-DTα and aqueous seed extract, respectively.



**Table 1** Results of antibacterial studies

Tested pathogens	Zone of inhibition (mm)			
	Zone-1 AgNO <sub>3</sub> (0.015 mg)	Zone-2 AgNP-DT <sub>a</sub> (0.01 mg)	Zone-3 AgNP-DT <sub>a</sub> (0.02 mg)	Zone-4 AgNP-DT <sub>a</sub> (0.03 mg)
<i>Klebsiella pneumonia</i>	19.5 ± 0.71	15.5 ± 0.71	17.25 ± 0.35	20 ± 00
<i>Staphylococcus aureus</i>	24.5 ± 0.71	20.5 ± 0.71	22.5 ± 0.71	36 ± 1.41
<i>Escherichia coli</i>	19.5 ± 0.71	15.5 ± 0.71	18.2 ± 0.35	19.5 ± 0.71
<i>Pseudomonas aeruginosa</i>	No clear zone	No clear zone	No clear zone	No clear zone

The values are expressed as mean ± SD.

aggregation. These non-aggregated nanoparticles are separated from each other by the bio-stabiliser. Therefore, these non-aggregated AgNP-DT<sub>a</sub> could interact strongly with the cell wall of bacteria because of their high surface energy and mobility; otherwise it would be lowered by the formation of large aggregates.<sup>63</sup> Also, DT stabilised nanoparticles have an average size of 16.05 ± 5.0 nm. Due to their small size they could easily reach the nuclear content of bacteria and their large surface areas increase the area of contact with bacteria than large sized nanoparticles.<sup>64</sup> From Fig. 6, it can be clearly recognized that green synthesized AgNP-DT<sub>a</sub> using DT were more active towards Gram positive *S. aureus* than other Gram negative bacteria. This might be because AgNP-DT<sub>a</sub> could easily bind with the proteins which crosslink peptidoglycans in the cell wall of Gram positive bacteria. Without the cell wall, a bacterial cell is vulnerable to osmosis causing the cell to swell and burst.<sup>65</sup> However, as-prepared AgNP-DT<sub>a</sub> also inhibit the growth of Gram negative bacteria such as *K. pneumonia* and *E. coli*. This may be because of the presence of oxidizable molecules on the surface of AgNP-DT<sub>a</sub> which can liberate free radicals and can cause cell death.<sup>66</sup> However, Gaillet *et al.* reported the potential of silver nanoparticles themselves to generate free radicals.<sup>67</sup> Conversely, newly synthesized AgNP-DT<sub>a</sub> did not inhibit the growth of *P. aeruginosa*; no clear zone was observed. The experiment was repeated with three month old AgNP-DT<sub>a</sub> and it showed negligible variations in the activity.

#### 4.5. *In vitro* antiproliferative activity of AgNP-DT<sub>a</sub>

The antiproliferative effects of the synthesized nanoparticles and DT extract were investigated using MTT assay on lung cancer cell line A549. The newly synthesized AgNP-DT<sub>a</sub> showed moderate activity on the A549 cell line Fig. 7. It was observed that the cytotoxic effect of AgNP-DT<sub>a</sub> on the cell line increased with the increase in the concentration of nanoparticles. The median effective concentration, EC 50 value, for cell mortality in A549 cell lines after exposure to DT synthesized AgNPs for 24 hours was found to be 86.23 ± 0.22 µg ml<sup>-1</sup>.

Moreover, the photographs of the cell cultures in Fig. 8 observed through an inverted phase contrast tissue culture microscope showed apoptotic changes and nuclear condensation induced on A549 by AgNP-DT<sub>a</sub>. The anti-proliferative

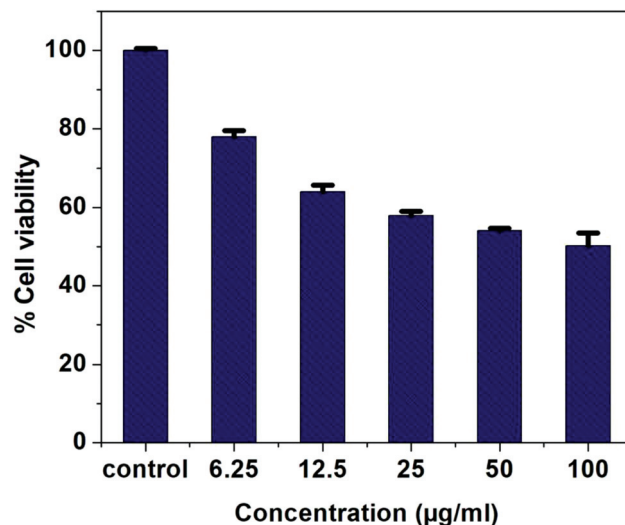


**Fig. 7** Plot showing the variation of % cell viability with the concentration of AgNP-DT<sub>a</sub>.

effect of the aqueous seed extract tested on the A549 cell line shows an EC 50 value higher than 100 µg ml<sup>-1</sup>. The activity of the as-prepared AgNP-DT<sub>a</sub> may be due to their relative stability which facilitates their penetration and survival in A549 tumour cells. AgNP-DT<sub>a</sub> may penetrate into cells and thus interfere with the proper functioning of cellular proteins and induce consequent changes in cellular chemistry.<sup>68</sup> Also, these non-aggregated, small sized AgNP-DT<sub>a</sub> are capable of developing reactive oxygen species (ROS) in the cells. Accumulation of ROS can cause oxidative stress, which can lead to DNA damage and substantial morphological changes in A549 and finally apoptotic cell death.<sup>69,70</sup> The median effective concentration, EC 50 value, of chemically synthesized silver nanoparticles using polyvinylpyrrolidone (PVP) for cell mortality in A549 cell lines was found to be 9.96 µg ml<sup>-1</sup>.<sup>71</sup> Hence our results confirmed that chemically synthesized silver nanoparticles led to more serious damage to cellular membrane compared to bio-capped AgNP-DT<sub>a</sub> synthesized using the ligands of DT. Thus we conclude that our newly synthesized AgNP-DT<sub>a</sub> show moderate anti-proliferative activity with less cytotoxicity compared to chemically synthesized silver nanoparticles.



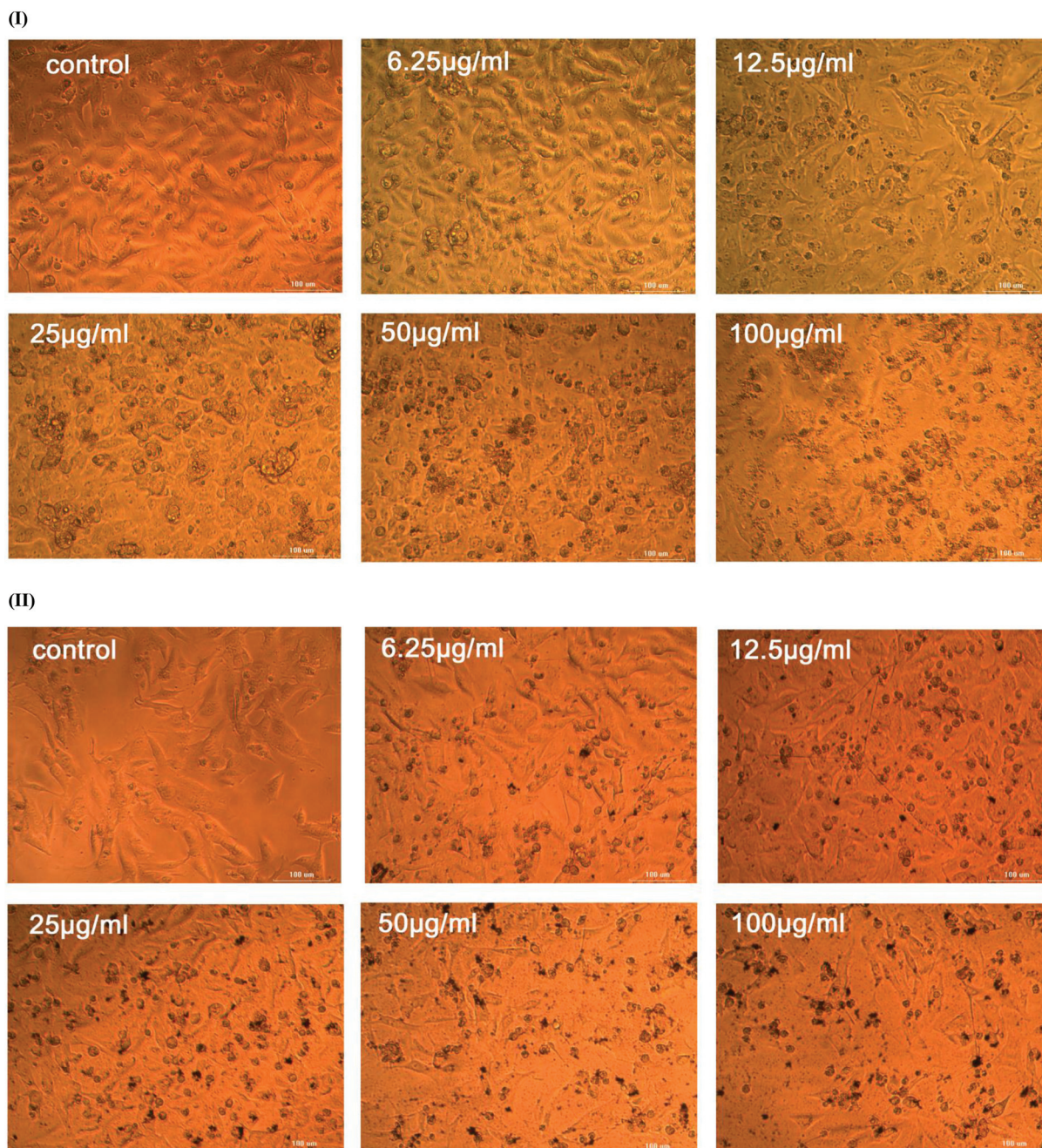


**Fig. 8** An inverted phase contrast tissue culture microscopy image of A549 cell lines on treatment with (I) a decoction of seeds of *DT* and (II) AgNP-DT $\alpha$ .

## 5. Conclusions

The present study focused on the application of the seeds of *DT*, a mangrove associated plant for a green-mediated synthesis of highly stable AgNP-DT $\alpha$ . The proposed method is a rapid, simple, inexpensive and environmentally safe approach. The synthesized metal nanoparticles were stable for over 3 months at room temperature and were well-dispersed in aqueous medium. The AgNP-DT $\alpha$  nanoparticles have narrow size distributions with an average size of  $16.05 \pm 5.0$  nm.

Interestingly, the as-prepared AgNP-DT $\alpha$  exhibited good antioxidant activity at low concentrations. The antioxidant capacity of AgNP-DT $\alpha$  was even relatively higher than that of Trolox, the reference compound. AgNP-DT $\alpha$  exhibited significant antibacterial potential against Gram positive and Gram negative bacteria. Hence they could be used as potential antibacterial agents in the food packing industry and in the medicinal field. In addition, AgNP-DT $\alpha$  showed moderate anti-proliferative activity on A549 lung cancer cell lines with a median effective concentration of  $86.23 \pm 0.22 \mu\text{g ml}^{-1}$  which is noteworthy.

## Conflicts of interest

The authors declare no conflicts of interest.

## Acknowledgements

The author (NC) is grateful to University Grants Commission (UGC), Government of India, New Delhi, India for providing financial assistance under the Faculty Development Programme (F.No.FIP/12th plan/KLMG034 TF13). The authors are thankful to Inter-University Instrumentation Centre (DST-SAIF & DST-FIST, Govt. of India) and School of Environmental Sciences, MGU (KSCSTE-SARD, VERC Project, Govt. of Kerala) for providing the instrumentation facility. The support and inspiration from Dr A. P. Thomas (Director, ACESSD) and Dr C. T. Aravindakumar (Professor, SES MGU) are gratefully acknowledged here. The authors are grateful to three anonymous reviewers for their critical comments which helped in further improvement of the manuscript.

## References

- 1 P. K. Jain, X. Huang, I. H. El-Sayed and M. A. El-Sayed, Noble metals on the nanoscale: optical and photothermal properties and some applications in imaging, sensing, biology, and medicine, *Acc. Chem. Res.*, 2008, **41**, 1578–1586.
- 2 M. S. Abdel-Aziz, M. S. Shaheen, A. A. El-Nekeety and M. A. Abdel-Wahhab, Antioxidant and antibacterial activity of silver nanoparticles biosynthesized using *Chenopodium murale* leaf extract, *J. Saudi Chem. Soc.*, 2014, **18**, 356–363.
- 3 S. Ahmed, G. Kaur, P. Sharma, S. Singh and S. Ikram, Evaluation of antioxidant, antibacterial and anticancer (lung cancer cell line A549) activity of *Punica granatum* mediated silver nanoparticles, *Toxicol. Res.*, 2018, **7**, 923–930.
- 4 J. S. Kim, E. Kuk, K. N. Yu, J.-H. Kim, S. J. Park, H. J. Lee, S. H. Kim, Y. K. Park, Y. H. Park and C.-Y. Hwang, Antimicrobial effects of silver nanoparticles, *Nanomedicine*, 2007, **3**, 95–101.
- 5 S. Ahmed, G. Kaur, P. Sharma, S. Singh and S. Ikram, Fruit waste (peel) as bio-reductant to synthesize silver nanoparticles with antimicrobial, antioxidant and cytotoxic activities, *J. Appl. Biomed.*, 2018, **16**, 221–231.
- 6 S. Ahmed, I. Zafeer and S. Ikram, One-step method for formation of silver nanoparticles using *Withania somnifera* extract for antimicrobial activities, *J. Bionanosci.*, 2016, **10**, 47–53.
- 7 S. Ahmed, K. Manzoor and S. Ikram, Synthesis of silver nanoparticles using leaf extract of *Crotalaria retusa* as Antimicrobial Green Catalyst, *J. Bionanosci.*, 2016, **10**, 282–287.
- 8 R. Sankar, A. Karthik, A. Prabu, S. Karthik, K. S. Shivashangari and V. Ravikumar, *Origanum vulgare* mediated biosynthesis of silver nanoparticles for its antibacterial and anticancer activity, *Colloids Surf., B*, 2013, **108**, 80–84.
- 9 T. Santhoshkumar, A. A. Rahuman, G. Rajakumar, S. Marimuthu, A. Bagavan, C. Jayaseelan, A. A. Zahir, G. Elango and C. Kamaraj, Synthesis of silver nanoparticles using *Nelumbo nucifera* leaf extract and its larvicidal activity against malaria and filariasis vectors, *Parasitol. Res.*, 2011, **108**, 693–702.
- 10 R. Chaturvedi and C. Jha, Standard manufacturing procedure of Rajata Bhasma, *AYU*, 2011, **32**, 566–571.
- 11 J. Lin, R. Chen, S. Feng, J. Pan, Y. Li, G. Chen, M. Cheng, Z. Huang, Y. Yu and H. Zeng, A novel blood plasma analysis technique combining membrane electrophoresis with silver nanoparticle-based SERS spectroscopy for potential applications in noninvasive cancer detection, *Nanomedicine*, 2011, **7**, 655–663.
- 12 P. Asharani, M. P. Hande and S. Valiyaveetil, Anti-proliferative activity of silver nanoparticles, *BMC Cell Biol.*, 2009, **10**, 65.
- 13 A. Ahmad, P. Mukherjee, S. Senapati, D. Mandal, M. I. Khan, R. Kumar and M. Sastry, Extracellular biosynthesis of silver nanoparticles using the fungus *Fusarium oxysporum*, *Colloids Surf., B*, 2003, **28**, 313–318.
- 14 N. Saifuddin, C. Wong and A. Yasumira, Rapid biosynthesis of silver nanoparticles using culture supernatant of bacteria with microwave irradiation, *J. Chem.*, 2009, **6**, 61–70.
- 15 J. Virkutyte and R. S. Varma, Green synthesis of metal nanoparticles: biodegradable polymers and enzymes in stabilization and surface functionalization, *Chem. Sci.*, 2011, **2**, 837–846.
- 16 S. P. Chandran, M. Chaudhary, R. Pasricha, A. Ahmad and M. Sastry, Synthesis of gold nanotriangles and silver nanoparticles using *Aloe vera* plant extract, *Biotechnol. Prog.*, 2006, **22**, 577–583.
- 17 H. Yoshimura, Protein-assisted nanoparticle synthesis, *Colloids Surf., A*, 2006, **282**, 464–470.
- 18 N. Aziz, M. Faraz, R. Pandey, M. Shakir, T. Fatma, A. Varma, I. Barman and R. Prasad, Facile algae-derived route to biogenic silver nanoparticles: synthesis, antibacterial, and photocatalytic properties, *Langmuir*, 2015, **31**, 11605–11612.
- 19 D. Mandal, M. E. Bolander, D. Mukhopadhyay, G. Sarkar and P. Mukherjee, The use of microorganisms for the formation of metal nanoparticles and their application, *Appl. Microbiol. Biotechnol.*, 2006, **69**, 485–492.
- 20 Y. Park, Y. Hong, A. Weyers, Y. Kim and R. Linhardt, Polysaccharides and phytochemicals: a natural reservoir for the green synthesis of gold and silver nanoparticles, *IET Nanobiotechnol.*, 2011, **5**, 69–78.
- 21 A. Ali and S. Ahmed, in *Handbook of Ecomaterials*, Springer, 2018, pp. 1–45.
- 22 X. Liu, B. Li, F. Fu, K. Xu, R. Zou, Q. Wang, B. Zhang, Z. Chen and J. Hu, Facile synthesis of biocompatible cysteine-coated CuS nanoparticles with high photothermal conversion efficiency for cancer therapy, *Dalton Trans.*, 2014, **43**, 11709–11715.



- 23 A. K. Mittal, D. Tripathy, A. Choudhary, P. K. Aili, A. Chatterjee, I. P. Singh and U. C. Banerjee, Bio-synthesis of silver nanoparticles using *Potentilla fulgens* Wall. ex Hook. and its therapeutic evaluation as anticancer and antimicrobial agent, *Mater. Sci. Eng., C*, 2015, **53**, 120–127.
- 24 N. Chanda, R. Shukla, A. Zambre, S. Mekapothula, R. R. Kulkarni, K. Katti, K. Bhattacharyya, G. M. Fent, S. W. Casteel and E. J. Boote, An effective strategy for the synthesis of biocompatible gold nanoparticles using cinnamon phytochemicals for phantom CT imaging and photoacoustic detection of cancerous cells, *Pharm. Res.*, 2011, **28**, 279–291.
- 25 K. P. Kumar, W. Paul and C. P. Sharma, Green synthesis of gold nanoparticles with *Zingiber officinale* extract: characterization and blood compatibility, *Process Biochem.*, 2011, **46**, 2007–2013.
- 26 L.-R. Xu, P. Zhou, Y.-E. Zhi, J. Wu and S. Zhang, Three new flavonol triglycosides from *Derris trifoliata*, *J. Asian Nat. Prod. Res.*, 2009, **11**, 79–84.
- 27 Y. Wang, W. Ma and W. Zheng, Deguelin, a novel anti-tumorigenic agent targeting apoptosis, cell cycle arrest and anti-angiogenesis for cancer chemoprevention, *Mol. Clin. Oncol.*, 2013, **1**, 215–219.
- 28 A. Yenesew, J. T. Kiplagat, S. Derese, J. O. Midiwo, J. M. Kabaruu, M. Heydenreich and M. G. Peter, Two unusual rotenoid derivatives, 7a-O-methyl-12a-hydroxy-deguelol and spiro-13-homo-13-oxaelliptone, from the seeds of *Derris trifoliata*, *Phytochemistry*, 2006, **67**, 988–991.
- 29 S. Tewtrakul, S. Cheenpracha and C. Karalai, Nitric oxide inhibitory principles from *Derris trifoliata* stems, *Phytomedicine*, 2009, **16**, 568–572.
- 30 S. Cheenpracha, C. Karalai, C. Ponglimanont and K. Chantrapromma, Cytotoxic rotenoloids from the stems of *Derris trifoliata*, *Can. J. Chem.*, 2007, **85**, 1019–1022.
- 31 A. Yenesew, H. Twinomuhwezi, J. M. Kabaruu, H. M. Akala, B. T. Kiremire, M. Heydenreich, M. G. Peter, F. Eyase, N. C. Waters and D. S. Walsh, Antiplasmodial and larvicidal flavonoids from *Derris trifoliata*, *Bull. Chem. Soc. Ethiop.*, 2009, **23**, 409–414.
- 32 A. Harborne, *Phytochemical methods a guide to modern techniques of plant analysis*, Springer Science & Business Media, 1998.
- 33 M. A. Hossain, K. A. S. AL-Raqmi, Z. H. AL-Mijizy, A. M. Weli and Q. Al-Riyami, Study of total phenol, flavonoids contents and phytochemical screening of various leaves crude extracts of locally grown *Thymus vulgaris*, *Asian Pac. J. Trop. Biomed.*, 2013, **3**, 705.
- 34 H. Usman, F. I. Abdulrahman and A. Usman, Qualitative phytochemical screening and in vitro antimicrobial effects of methanol stem bark extract of *Ficus thonningii* (Moraceae), *Afr. J. Tradit., Complementary Altern. Med.*, 2009, **6**, 289–295.
- 35 N. L. Conklin-Brittain, E. S. Dierenfeld, R. W. Wrangham, M. Norconk and S. Silver, Chemical protein analysis: a comparison of Kjeldahl crude protein and total ninhydrin protein from wild, tropical vegetation, *J. Chem. Ecol.*, 1999, **25**, 2601–2622.
- 36 N. Jaradat, F. Hussien and A. Al Ali, Preliminary phytochemical screening, quantitative estimation of total flavonoids, total phenols and antioxidant activity of *Ephedra alata* Decne., *J. Mater. Environ. Sci.*, 2015, **6**, 1771–1778.
- 37 K. L. Singh and G. Bag, Phytochemical analysis and determination of total phenolics content in water extracts of three species of *Hedychium*, *Phytochem. Anal.*, 2013, **5**, 1516–1521.
- 38 V. L. Singleton, R. Orthofer and R. M. Lamuela-Raventós, in *Methods in Enzymology*, Academic Press, 1999, vol. 299, pp. 152–178.
- 39 R. Aquino, S. Morelli, M. R. Lauro, S. Abdo, A. Saija and A. Tomaino, Phenolic Constituents and Antioxidant Activity of an Extract of *Anthurium versicolor* Leaves, *J. Nat. Prod.*, 2001, **64**, 1019–1023.
- 40 P. Prieto, M. Pineda and M. Aguilar, Spectrophotometric quantitation of antioxidant capacity through the formation of a phosphomolybdenum complex: specific application to the determination of vitamin E, *Anal. Biochem.*, 1999, **269**, 337–341.
- 41 S. Irshad, M. Mahmood and F. Perveen, In vitro antibacterial activities of three medicinal plants using agar well diffusion method, *Res. J. Biol.*, 2012, **2**, 1–8.
- 42 K. Muthu and S. Priya, Green synthesis, characterization and catalytic activity of silver nanoparticles using *Cassia auriculata* flower extract separated fraction, *Spectrochim. Acta, Part A*, 2017, **179**, 66–72.
- 43 J. Zheng and R. M. Dickson, Individual water-soluble dendrimer-encapsulated silver nanodot fluorescence, *J. Am. Chem. Soc.*, 2002, **124**, 13982–13983.
- 44 T. Chen and Y. Liu, *Semiconductor Nanocrystals and Metal Nanoparticles: Physical Properties and Device Applications*, CRC Press, 2016.
- 45 C. Mihalcea, D. Büchel, N. Atoda and J. Tominaga, Intrinsic fluorescence and quenching effects in photoactivated reactively sputtered silver oxide layers, *J. Am. Chem. Soc.*, 2001, **123**, 7172–7173.
- 46 M. Nasrollahzadeh, S. M. Sajadi, E. Honarmand and M. Maham, Preparation of palladium nanoparticles using *Euphorbia thymifolia* L. leaf extract and evaluation of catalytic activity in the ligand-free Stille and Hiyama cross-coupling reactions in water, *New J. Chem.*, 2015, **39**, 4745–4752.
- 47 V. Vidhu and D. Philip, Spectroscopic, microscopic and catalytic properties of silver nanoparticles synthesized using *Saraca indica* flower, *Spectrochim. Acta, Part A*, 2014, **117**, 102–108.
- 48 V. Vidhu and D. Philip, Catalytic degradation of organic dyes using biosynthesized silver nanoparticles, *Micron*, 2014, **56**, 54–62.
- 49 D. Kang and M. Trenary, Surface chemistry of ethylenediamine (NH<sub>2</sub>CH<sub>2</sub>CH<sub>2</sub>NH<sub>2</sub>) on Pt (1 1 1), *Surf. Sci.*, 2000, **470**, L13–L19.
- 50 W. Zheng and S. Y. Wang, Antioxidant activity and phenolic compounds in selected herbs, *J. Agric. Food Chem.*, 2001, **49**, 5165–5170.



- 51 H. Tohma, İ. Gülçin, E. Bursal, A. C. Gören, S. H. Alwasel and E. Köksal, Antioxidant activity and phenolic compounds of ginger (*Zingiber officinale* Rosc.) determined by HPLC-MS/MS, *J. Food Meas. Charact.*, 2017, **11**, 556–566.
- 52 A. C. de Camargo, M. A. B. Regitano-d'Arce, G. B. Rasera, S. G. Canniatti-Brazaca, L. do Prado-Silva, V. O. Alvarenga, A. S. Sant'Ana and F. Shahidi, Phenolic acids and flavonoids of peanut by-products: Antioxidant capacity and antimicrobial effects, *Food Chem.*, 2017, **237**, 538–544.
- 53 F. M. Roleira, E. J. Tavares-da-Silva, C. L. Varela, S. C. Costa, T. Silva, J. Garrido and F. Borges, Plant derived and dietary phenolic antioxidants: anticancer properties, *Food Chem.*, 2015, **183**, 235–258.
- 54 A. Dalar, Y. Guo and I. Konczak, Phenolic composition and potential anti-inflammatory properties of *Verbascum cheiranthifolium* var. *cheiranthifolium* leaf, *J. Herb. Med.*, 2014, **4**, 195–200.
- 55 K. Lo and P. C. Cheung, Antioxidant activity of extracts from the fruiting bodies of *Agrocybe aegerita* var. *alba*, *Food Chem.*, 2005, **89**, 533–539.
- 56 K. Niraimathi, V. Sudha, R. Lavanya and P. Brindha, Biosynthesis of silver nanoparticles using *Alternanthera sessilis* (Linn.) extract and their antimicrobial, antioxidant activities, *Colloids Surf., B*, 2013, **102**, 288–291.
- 57 L. Inbathamizh, T. M. Ponnu and E. J. Mary, In vitro evaluation of antioxidant and anticancer potential of *Morinda pubescens* synthesized silver nanoparticles, *J. Pharm. Res.*, 2013, **6**, 32–38.
- 58 T. Yokozawa, C. P. Chen, E. Dong, T. Tanaka, G.-I. Nonaka and I. Nishioka, Study on the inhibitory effect of tannins and flavonoids against the 1, 1-diphenyl-2-picrylhydrazyl radical, *Biochem. Pharmacol.*, 1998, **56**, 213–222.
- 59 S. Bhakya, S. Muthukrishnan, M. Sukumaran and M. Muthukumar, Biogenic synthesis of silver nanoparticles and their antioxidant and antibacterial activity, *Appl. Nanosci.*, 2016, **6**, 755–766.
- 60 S. Francis, S. Joseph, E. P. Koshy and B. Mathew, Microwave assisted green synthesis of silver nanoparticles using leaf extract of *Elephantopus scaber* and its environmental and biological applications, *Artif. Cells, Nanomed., Biotechnol.*, 2018, **46**, 795–804.
- 61 S. Torres, V. Campos, C. León, S. Rodríguez-Llamazares, S. Rojas, M. Gonzalez, C. Smith and M. Mondaca, Biosynthesis of selenium nanoparticles by *Pantoea agglomerans* and their antioxidant activity, *J. Nanopart. Res.*, 2012, **14**, 1236.
- 62 W. Cai, T. Hu, A. M. Bakry, Z. Zheng, Y. Xiao and Q. Huang, Effect of ultrasound on size, morphology, stability and antioxidant activity of selenium nanoparticles dispersed by a hyperbranched polysaccharide from *Lignosus rhinocerotis*, *Ultrason. Sonochem.*, 2018, **42**, 823–831.
- 63 L. Kvitek, A. Panáček, J. Soukupova, M. Kolář, R. Večeřová, R. Prucek, M. Holecova and R. Zbořil, Effect of surfactants and polymers on stability and antibacterial activity of silver nanoparticles (NPs), *J. Phys. Chem. C*, 2008, **112**, 5825–5834.
- 64 G. Martinez-Castanon, N. Nino-Martinez, F. Martinez-Gutierrez, J. Martinez-Mendoza and F. Ruiz, Synthesis and antibacterial activity of silver nanoparticles with different sizes, *J. Nanopart. Res.*, 2008, **10**, 1343–1348.
- 65 W. W. Navarre and O. Schneewind, Surface proteins of gram-positive bacteria and mechanisms of their targeting to the cell wall envelope, *Microbiol. Mol. Biol. Rev.*, 1999, **63**, 174–229.
- 66 T. Miller, Killing and lysis of Gram-negative bacteria through the synergistic effect of hydrogen peroxide, ascorbic acid, and lysozyme, *J. Bacteriol.*, 1969, **98**, 949–955.
- 67 S. Gaillet and J.-M. Rouanet, Silver nanoparticles: their potential toxic effects after oral exposure and underlying mechanisms—a review, *Food Chem. Toxicol.*, 2015, **77**, 58–63.
- 68 J. V. Rogers, C. V. Parkinson, Y. W. Choi, J. L. Speshock and S. M. Hussain, A preliminary assessment of silver nanoparticle inhibition of monkeypox virus plaque formation, *Nanoscale Res. Lett.*, 2008, **3**, 129.
- 69 P. F. Li, R. Dietz and R. Von Harsdorf, p53 regulates mitochondrial membrane potential through reactive oxygen species and induces cytochrome c-independent apoptosis blocked by Bcl-2, *EMBO J.*, 1999, **18**, 6027–6036.
- 70 S. Gurunathan, J. Raman, S. N. A. Malek, P. A. John and S. Vikineswary, Green synthesis of silver nanoparticles using *Ganoderma neo-japonicum* Imazeki: a potential cytotoxic agent against breast cancer cells, *Int. J. Nanomed.*, 2013, **8**, 4399.
- 71 W. Liu, Y. Wu, C. Wang, H. C. Li, T. Wang, C. Y. Liao, L. Cui, Q. F. Zhou, B. Yan and G. B. Jiang, Impact of silver nanoparticles on human cells: effect of particle size, *Nanotoxicology*, 2010, **4**, 319–330.